npj | computational materials

Article

Published in partnership with the Shanghai Institute of Ceramics of the Chinese Academy of Sciences

https://doi.org/10.1038/s41524-024-01244-3

The Bell-Evans-Polanyi relation for hydrogen evolution reaction from first-principles

Timothy T. Yang [1,2] & Wissam A. Saidi [1,2] ✉

The versatile Bell-Evans-Polanyi (BEP) relation stipulates the kinetics of a reaction in terms of thermodynamics. Herein, we establish the BEP relation for the hydrogen evolution reaction (HER) from fundamental electrochemical principles leveraging the Butler-Volmer relation for a one-step, one-electron process and the transition state theory. Based on first-principles investigations of HER mechanisms on fourteen metal electrodes, we firmly justify the BEP relation solely using an easy-to compute hydrogen adsorption free energy and universal electrochemical constants.

Descriptor-based approaches carry enormous predictive power in materials design as these can be rapidly deployed to identify materials with desired properties[1–8]. The empirical Bell (Brønsted)-Evans-Polanyi (BEP) relationship (Brøonsted and Pederson recognized the BBEP relation from studying the decomposition of nitroamide catalyzed by series of anionic bases in aqueous, and was later derived individually by Bell, and by Evan and Polanyi. Generally referred as Bell (Brønsted)-Evans-Polanyi relation)[9–14], – a linear trend between the activation energy and the reaction energy of a given process, has been widely employed to stipulate reaction kinetics based on easy-to-compute or easily-accessible thermodynamic data[15–20]. In the past two decades, BEP relationships have been widely observed for different reactions such as the dissociation of diatomic and triatomic molecules[21–24].

Hydrogen evolution reaction (HER) is the critical step in electrolysis to produce green hydrogen, which is considered a next-generation clean energy carrier[25,26]. Leveraging the BEP relation as the key ingredient for computational screening of HER catalysts, Nørskov et al. proposed the hydrogen adsorption free energy ΔG_H as the descriptor for the volcano trend – the logarithm of the exchange current is linearly increasing or decreasing with ΔG_H[27]. Such behavior is in line with the Sabatier's principle, which stipulates that the optimum reaction rates that correspond to moderate adsorption strength between catalysts and reactants. Recent first-principles computational studies have shown that the BEP relation holds for HER on metal surfaces[28,29]. Experimentally, similar trends were also shown to be valid by studying the cyclic voltammograms on metal surfaces under varying electrochemical conditions[30,31]; namely, the logarithm of the exchange current was found to linearly correlate with the hydrogen binding energy which was determined from the desorption peak potential or with the HER onset potential. However, the BEP relation has been demonstrated using various kinetic and thermodynamic descriptors. Such different measures underscore its empirical nature, and calls for deeper understanding of its roots and connections, if any, with fundamental electrochemistry at the atomic level.

This study presents a derivation of the BEP relation for HER based on the theoretical Butler-Volmer relation – the norm of the electrochemical theory that describes current-potential characteristics for electrochemical reactions. Utilizing the *absolute form of the standard rate constant* that follows the transition state theory, we not only correlate between HER thermodynamics and kinetics, but further quantify the BEP relationship solely with the easy-to-compute hydrogen adsorption free energy ΔG_H and *universal* electrochemical constants. Further, we verify the BEP relation using first-principles calculations by finding a direct correlation between the activation free energy of the rate-determining step (rds) and the hydrogen adsorption energy on fourteen metal electrode surfaces. Last, we show that the BEP relation can be utilized to reproduce experimental exchange currents for a wide variety of catalysts with HER activities that vary by 10 orders of magnitude.

Results

Derivation of the Bell-Evans-Polanyi relation

Hydrogen evolution reaction $H^+ + e^- \rightarrow \frac{1}{2}H_2$ is the cathodic reaction in water splitting. In acidic environments, HER takes place through the Volmer–Heyrovsky or Volmer–Tafel pathways,

$$H_3O^+ + e^- \leftrightarrow H^* + H_2O \quad \text{(Volmer)}$$

$$H_3O^+ + e^- + H^* \leftrightarrow H_2O + H_2 \quad \text{(Heyrovsky)}$$

$$H^* + H^* \leftrightarrow H_2 \quad \text{(Tafel)}$$

[1]Department of Materials Science and Engineering, University of Pittsburgh, Pittsburgh, PA 15260, USA. [2]Department of Energy, National Energy Technology Laboratory, Pittsburgh, PA 15236, USA. ✉e-mail: wissam.saidi@netl.doe.gov

Similar steps exist in alkaline mediums but will not be discussed further[32]. The Volmer reaction describes the reduction of hydrogen ions H^+ on an electrode surface, whereas the Heyrovsky process describes the reduction of H^+ and its interaction with an adsorbed hydrogen atom H^* to form hydrogen gas H_2 (g). The Tafel reaction is the formation of H_2(g) through combining adsorbed hydrogen atoms.

Assuming that $H^+ + e^- \rightarrow \frac{1}{2}H_2$ is primarily determined by the rds, involving proton reduction $H^+ + e^- \rightarrow H$[17], we can write the current density as $j = e[C_{H^+} r_f - C_H r_b]$ where $r_{f/b}$ is the rate for the forward/backward redox reaction. C_{H^+} and C_H are the concentration of H^+ and H near the electrode surface, respectively. Such description for the overall HER current is justified under the condition that the proton reduction follows a consecutive step with a negligible activation barrier to be either stabilized on the surface or to form H_2 molecule for the Volmer or Heyrovsky reaction, respectively. This is confirmed by first-principles modeling of minimum reaction pathways, as will be discussed later on. Using the Butler-Volmer relation for a *one-step, one electron* transfer process, we write the reaction rates as,

$$\begin{cases} r_f = k_f \exp\left[-\alpha f\left(E - E^{0'}\right)\right] \\ r_b = k_b \exp\left[(1-\alpha) f\left(E - E^{0'}\right)\right] \end{cases}, \tag{1}$$

where α and $E^{0'}$ are respectively the transfer coefficient and the formal potential for the redox process of the rds, and E is the applied potential; $k_{f/b}$ is the forward/backward reaction rate constant and $f = F/RT$ where F is the Faraday's constant, R is the gas constant and T is the temperature. Thus, we can express the current density as,

$$j = e\left\{C_{H^+} k_f \exp[-\alpha f\left(E - E^{0'}\right)] - C_H k_b \exp[(1-\alpha) f\left(E - E^{0'}\right)]\right\}. \tag{2}$$

At the overall HER equilibrium potential E_{eq} where the forward current density is the same as the backward current density, the exchange current density is defined as,

$$j_0 = eC_{H^+} k_0 \exp[-\alpha f(E_{eq} - E^{0'})] = eC_H k_0 \exp[(1-\alpha) f(E_{eq} - E^{0'})]. \tag{3}$$

Here, k_0 is the standard rate constant defined under the condition that the forward r_f or the backward r_b rates are the same at E_{eq}, i.e., $k_0 = k_f = k_b$[33]. Under the assumption that all the elementary steps are at equilibrium if the overall reaction is at equilibrium, as it has been proven theoretically[33], we obtain the following (see SI for the detailed derivation):

$$E_{eq} - E^{0'} = \begin{cases} \Delta G_H/|e| & \text{(Volmer)} \\ -\Delta G_H/|e| & \text{(Heyrovsky)} \end{cases} \tag{4}$$

Here, ΔG_H is defined as the free energy difference between the hydrogen at the adsorbed and gas states. It can be quantified from density functional theory (DFT) calculations, as shown in Eq. (9).

The critical step in deriving the BEP relation is to utilize the *absolute form of the standard rate constant* $k_0 = \frac{k_B T}{h} \exp(-\Delta G_0^+ / k_B T)$, which has long been considered empirical using a data-driven approach based on experimental data[21]. This form is in agreement with the Eyring's interpretation where the pre-factor of a chemical reaction is mainly $\frac{k_B T}{h}$, and the reaction rate is dominated by the exponential of the energy difference between the transition and initial state[34–36]. In our previous studies, we find that $\Delta G_0^+ = 0.7$ eV is universal, and is the overall HER activation barrier for the optimum catalysts with $\Delta G_H = 0$[37,38]. Similar values are found for the activation energy barriers of the Volmer, Heyrovsky and Tafel reactions on Pt (111) surface using DFT calculations[38]. Further, this absolute form of k_0 is verified by applying Eq. (3) to experimental exchange currents for metal surfaces[37,39]. Using the absolute form of k_0 and applying Eq. (4) into Eq. (3), we can re-express the first term of Eq. (3) as,

$$j_0 = \begin{cases} eC_{H^+} \frac{k_B T}{h} \exp\left(-\frac{\Delta G_0^+ + \alpha \Delta G_H}{k_B T}\right) & \text{(Volmer)} \\ eC_{H^+} \frac{k_B T}{h} \exp\left(-\frac{\Delta G_0^+ - \alpha \Delta G_H}{k_B T}\right) & \text{(Heyrovsky)} \end{cases} \tag{5}$$

Equation (5) has the Arrhenius form for an activation process,

$$j_0 = eC_{H^+} \frac{k_B T}{h} \exp(-\Delta G_{tot}^+ / k_B T), \tag{6}$$

provided that we define an "acting" or effective activation energy ΔG_{tot}^+ as,

$$\Delta G_{tot}^+ = \begin{cases} \Delta G_0^+ + \alpha \Delta G_H & \text{(Volmer)} \\ \Delta G_0^+ - \alpha \Delta G_H & \text{(Heyrovsky)} \end{cases} \tag{7}$$

Based on fundamental electrochemistry principles and the transition state theory, the derived Eq. (7) provides a universal and direct link between the thermodynamics and kinetics of HER. Importantly, ΔG_{tot}^+ can be quantified solely using ΔG_H that can be readily accessed from DFT[27]. Hence, we posit that Eq. (7) explains the BEP relationship that will be further verified and elucidated using DFT, as detailed below.

While the physical interpretation of ΔG_{tot}^+ is not clear from the derivation, we posit that ΔG_{tot}^+ is the activation free energy of the proton reduction of the rds. To show this is the case, we investigate the HER kinetics and thermodynamics using first-principles calculations on fourteen different metal surfaces including metals with moderate (Pt, Ir, Pd and Rh), strong (Re, Ru, Co and Ni) and light (Cu, Au, Ag, In, Cd and Bi) interactions with hydrogen. These metals are of high interest for materials design, and their electrochemical properties for catalyzing HER have been thoroughly studied[37,39,40]. We employ the Helmholtz double-layer model constructed using a water monolayer layer, with 1/8 proton concentration, placed ~3 Å above the metal surface[41]. For the metals with $Fm\bar{3}m$ and P63/mmc symmetry[42,43], we use (111) and (001) termination, respectively; for Bi and In, we use (111) termination[44]. In the water monolayer, each H_3O^+ molecule is bonded with three H_2O molecules in the Eigen form[45]. Similar to what was done for Pt (111)[46], the water molecules are arranged in an ice-like configuration, involving half of H_2O molecules with their O-H bonds perpendicular to the surface, while the other half are parallel to the surface, referenced to their molecular plane.

BEP validation

Using ΔG_H obtained from Eq. (9), we compute ΔG_{tot}^+ from Eq. (7) with the universal parameters $\Delta G_0^+ = 0.7$ eV and $\alpha = 0.5$. As shown in Fig. 1a, $\Delta G_{tot}^+ \approx \Delta G_{DFT}^+$ within ±0.2 eV uncertainties, strongly supporting that the acting ΔG_{tot}^+ can be interpreted as the activation free energy of the rds for the overall HER reaction. We further show that $\Delta G_{tot}^+ \approx \Delta G_{exp}^+$ where ΔG_{exp}^+ is computed from Eq. (7) with the values of $\alpha = 0.52 \pm 0.15$ and $\Delta G_0^+ = 0.69 \pm 0.10$ eV obtained from analyzing the experimental cyclic voltammograms of the fourteen metals using Eq. (2)[40]. The finding $\Delta G_{tot}^+ \approx \Delta G_{DFT}^+ \approx \Delta G_{exp}^+$ suggests the self-consistency of the BEP relationship of Eq. (7), and can further be confirmed by establishing statistical significance. In Fig. 1b, we individually fit the two trends from Fig. 1a with the BEP relation of Eq. (7) assuming that α and ΔG_0^+ as fitting parameters. The fitted α values are found 0.55 and 0.53, and the fitted ΔG_0^+ is 0.66 for both trends. The high coherency of the coefficient of determination r^2 values (0.88 and 0.87) confirms our previous findings of the *absolute reaction rate* as well as showing that $\alpha \approx 0.5$ can be treated as the universal value for all surfaces[37,39,40]. Importantly, we have confirmed our assumption that $\Delta G_{tot}^+ \approx \Delta G_{DFT}^+$ corresponds to the activation free energy of the proton transfer of the rds that can be obtained from first-principles modeling.

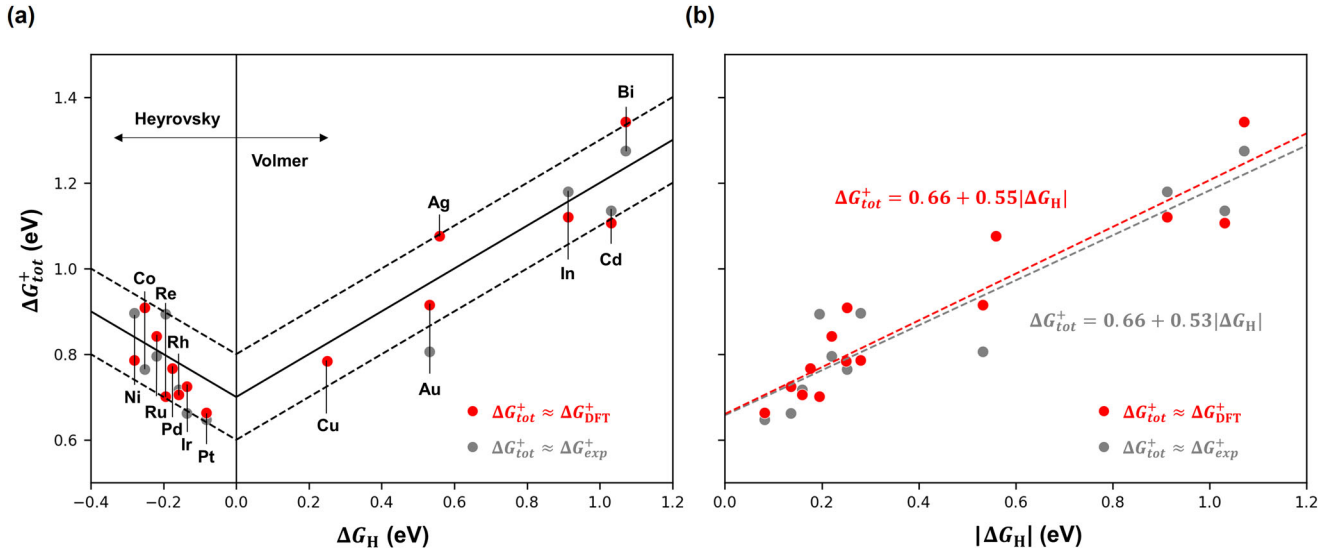

Fig. 1 | Correlation between the activation energy and the hydrogen adsorption free energy. a The trend of ΔG^+_{tot} with the computed ΔG_H. ΔG^+_{DFT} is computed from first principles modeling (red scatters) and ΔG^+_{exp} is calculated from Eq. (7) with the α and ΔG^+_0 values obtained from experimental cyclic voltammograms (gray). The black line is computed using Eq. (7) with the universal values of $\Delta G^+_0 = 0.7$ eV and $\alpha = 0.5$, and the black dashed lines are the boundaries of ±0.1 eV difference of ΔG^+_{tot}. **b** The fittings of ΔG^+_{DFT} and ΔG^+_{exp} with the BEP relation of Eq. (7). For the DFT and the experimental sets, the r^2 values are 0.88 and 0.87, respectively.

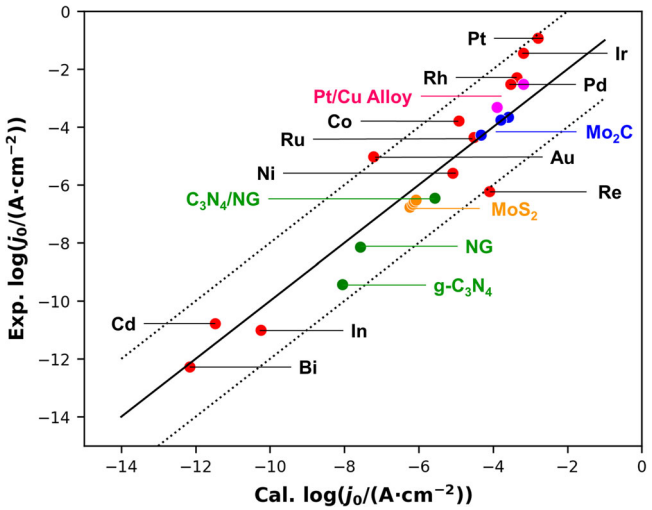

Fig. 2 | Correlation between the calculated and the experimental exchange current density. Comparison of the experimental j_0 and the calculated j_0 using Eq. (8) with the universal values $\Delta G^+_0 = 0.7$ eV and $\alpha = 0.5$. The solid line shows parity and the dashed lines are the boundaries of the difference within two orders of magnitude.

Discussion

Figure 1a shows the linear trend where ΔG^+_{DFT} increases with increasing or decreasing ΔG_H for the cases of the Volmer ($\Delta G_H > 0$) or the Heyrovsky ($\Delta G_H < 0$) reaction. Previous findings of the linear trends between ΔG_H and the activation free energies are qualitatively in line with our findings while the activation free energies are defined differently. For example, Cheng et al. used an implicit solvation model[47] to study the activation free energy defined at 0.5 vs. NHE for hollow or atop sites[28], which is different from our computed ΔG^+_{DFT} that is determined at 0 vs. NHE. Also, using NEB with the potential correction scheme[48], Tang et al. referenced the activation free energy to the protons in bulk solution[29], which is also different from ΔG^+_{DFT} that is referenced to the protons near electrode surface. Different from these previous studies where the linear trends are built with fitting parameters with no connection to theory, our theoretical BEP relation of Eq. (7), that follows naturally from fundamental electrochemical principles, is established with the well-defined ΔG_H, ΔG^+_0 and the electrochemical quantity α.

The BEP relation of Eq. (7) can be applied to quantify the exchange current j_0 for catalysts solely from computing ΔG_H in conjunction with Eq. (6). For the Volmer reaction, we approximate $C_{H^+} = C_{tot}(1-\theta)$ as H^+ is closely in contact with the empty stable sites for adsorption process, where C_{tot} is the areal concentration of total active sites and θ is the hydrogen adsorption fraction. For the Heyrovsky reaction, we approximate $C_{H^+} = C_{tot}\theta$ as H_2 formation must associate with an adsorbed hydrogen atom. This is based on the assumption that there is no mass transfer effects, as discussed in SI. Thus, we can rewrite Eq. (6) as,

$$j_0 = \begin{cases} eC_{tot}(1-\theta)\frac{k_B T}{h}\exp(-\Delta G^+_{tot}/k_B T) & \text{(Volmer)} \\ eC_{tot}\theta\frac{k_B T}{h}\exp(-\Delta G^+_{tot}/k_B T) & \text{(Heyrovsky)} \end{cases} \quad (8)$$

where ΔG^+_{tot} follows Eq. (7) with the universal parameters $\Delta G^+_0 = 0.7$ eV and $\alpha = 0.5$. Further, we use the Langmuir isotherm $\theta = K/(1+K)$ with the equilibrium constant $K = \exp(-\Delta G_H/k_B T)$, which has been confirmed to be a suitable approximation on metal surfaces based on ab initio thermodynamics (see SI). Note that the heterogeneous nature of the adsorption sites on realistic electrodes violates the Langmuir isotherm that describes the homogeneous adsorption events. However, nevertheless, this model has been shown to provide a reasonable approximation for experimental exchange currents[27,37,39].

Figure 2 compares the experimental j_0 and the j_0 calculated using Eq. (8) for fourteen metal surfaces. As seen from the figure, the differences between the experimental and calculated j_0 are within two orders of magnitude. Further, we posit that the BEP relation is general and is not only limited to pure metal surfaces. This is supported by examining a variety of catalysts with different structures and activities. Namely, (1) Pt/Cu surface alloys and near-surface alloys[49], (2) pristine, Ti- and Ir-doped β-Mo_2C[50], (3) MoS_2 nanoparticles supported on Au (111) with different loadings[51], (4) two dimensional metal free catalysts such as nitrogen doped graphene (NG), g-C_3N_4, and C_3N_4/NG hybrid[52]. These studies are selected based on: (1) the reported ΔG_H corresponds to the active sites that dominantly contribute to the overall HER, and (2) the concentration of the active sites $C_{tot} \approx N_{site}/A_{surf}$ can be estimated by the reported information, where N_{site} is the number of active sites and A_{surf} is the surface area. For 3-dimentional electrodes such as metals and β-Mo_2C, we approximate N_{site} using the most stable termination with the active sites that are determined using ab initio thermodynamics[53]. For N-G, we consider

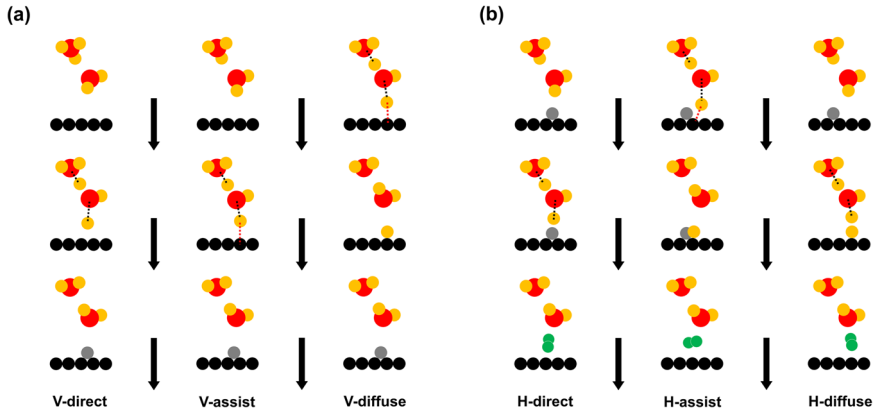

Fig. 3 | The routes for the elementary steps of the hydrogen evolution reaction. Schematic of potential routes for the (**a**) Volmer reaction and (**b**) Heyrovsky reaction. The oxygen and hydrogen atoms are shown in red and yellow, respectively. The surface hydrogen atoms on the stable/non-stable sites are shown in gray/yellow. The electrode surface metal atoms are shown in black. The stretched O-H bonds are represented by black dashed lines, and the red dashed lines represent the interaction of a hydrogen atom with a surface metal atom.

the reported doping percentage of 6.2% for determining the number of active sites shown to be the atop sites near the doped N atoms[52]. For C_3N_4@NG and G-C_3N_4, N_{site} is assumed to be the number of the bridge sites of N atoms[52]. The N_{site} for MoS_2 is calculated based on the reported densities of active Mo-edge sites[51]. As shown in the figure, the compute j_0 values are in line with the experimental values for all the investigated electrodes despite the differences of 10 orders of magnitude in the exchange currents. This suggests that one can easily screen the experimental j_0 with high fidelity using the easy-to-compute ΔG_H without conducting the high-cost investigations of reaction kinetic under electrochemical conditions.

In summary, we derive the BEP relation of the hydrogen evolution reaction – the linear trend between the activation energy and the reaction energy. From the Butler-Volmer (BV) relation - the empirical equation that explains the relation between electrochemical current and potential using the fundamentals of electrochemistry, we identify that the activation energy of the electrochemical current ΔG^+_{tot} is linearly proportional to, and solely a function of the DFT-based hydrogen adsorption free energy ΔG_H. This is done by introducing the *absolute form of the standard rate constant* into the BV equation and describing the electrochemical potential using ΔG_H. To further confirm the BEP relation, we employ first-principles modeling to compute the kinetic barriers of the minimum reaction pathways in conjunction with a charge transfer correction scheme to quantify ΔG^+_{tot}. We show that the ΔG^+_{tot} values computed using first principles are in agreement with the values obtained from experimental cyclic voltammograms. Last, we show that the BEP relation can be utilized to compute the exchange current with high fidelity solely using ΔG_H for a variety of electrodes. Our framework of building the theoretical BEP relation is general and is applicable for other reactions.

Methods

Computational hydrogen adsorption free energy

Employing the Helmholtz double-layer models, we compute the hydrogen adsorption free energy as,

$$\Delta G_H = \Delta E_{ads} + \Delta E_{ZPE} - T\Delta S, \tag{9}$$

where ΔE_{ZPE} is the zero-point energy difference between hydrogen in adsorbed state H and gas state H_2(g), and is approximately 0.04 eV[27]. At T= 298 K, we use experimental results to estimate the entropic contribution $T\Delta S \approx -0.2$ eV, as done before[54]. The adsorption energy is defined as $\Delta E_{ads} = \frac{1}{n}(E_{nH/slab} - E_{slab} - 0.5nE_{H_2(g)}) + \Delta E_{H_2O}$ where $E_{nH/slab}$ and E_{slab} are respectively the DFT energies of the surface with n adsorbed hydrogen and of the empty slab, and $E_{H_2(g)}$ is the energy of H_2 molecule in the gas phase. The solvation energy ΔE_{H_2O} due to surface-water interactions are found to be less than 0.1 eV. The reaction that is rate limiting can be *apriori* screened by examining ΔG_H: the rds is the Volmer or the Heyrovsky reaction for $\Delta G_H > 0$ or $\Delta G_H < 0$, respectively. Such justification was first confirmed by a first-principles study of the reaction pathways on metal surfaces[29]. Also, this is consistent with our previous studies on the exchange current model based on the theoretical Butler-Volmer relation[37,39].

Computational activation energy

We employ the nudged elastic band theory (NEB)[55] to search for the minimum reaction pathways of the rds. From a careful security, we investigate three different routes for each of the rds, as shown schematically in Fig. 3. We note that these reaction paths were not fully investigated in previous studies, see e.g., refs. 38,56 As shown in Fig. 3, all the reaction routes commence by transferring a hydrogen atom, referred as H_{tran}, from water layer to surface, but they differ by the nature of the active site(s) associated with charge transfer. For the Volmer reaction, the three potential routes correspond to,

I. H_{tran} directly adsorbs at the most stable site (V-direct).
II. H_{tran} adsorbs at the most stable site along a tilted path after slightly bonding to a surface metal atom (V-assist).
III. H_{tran} initially adsorbs at an unstable site (the top site of a surface atom, i.e., the atop site), then diffuses to the most stable adsorption site (V-diffuse).

For the Heyrovsky reaction, the three routes are,

I. H_{tran} directly interacts with H* to form H_2 without interacting with a surface site (H-direct).
II. H_{tran} combines with an H* to form H_2 after slightly bonding with a surface metal atom at an unstable site (atop site) (H-assist).
III. H_{tran} directly combines with an H* that diffuses from the most stable site to an unstable site (atop site) without interacting with a surface site (H-diffuse).

As shown in Supplementary Table 1, the favorable routes for the Volmer or Heyrovsky reactions differ across various metal surfaces. For example, Ru, Ir and Pt follow H-direct, H-assist and H-diffuse routes for the Heyrovsky reaction, respectively. From these investigations, we obtain the barrier of the minimum reaction pathways ΔE^+_{DFT} with an initial state where the protons are near the electrode surface. The initial state is distinguished from another study where it is referenced with respect to the protons in bulk solution[29]. We further correct ΔE^+_{DFT} by $\Delta q\left[\frac{1}{2}\Delta\phi - (\phi_{SHE} - \phi_I)\right]$ following an extrapolation scheme[48] to account for the varying potential along the reaction pathways as imposed by the periodic supercell model. Here, $\Delta\phi = \phi_T - \phi_I$ is the change of the work function from the initial (I) to transition state (T), and $\Delta q = q_T - q_I$ is the difference in excess surface charge between the two states, respectively. The excess surface charge $q = q_{water} - q_{surf}$ is determined using the Bader charge analysis[48], where q_{water} is the total charge of an isolated water layer and $q_{water/surf}$ is the total surface charge of the water layer in contact with the surface. To extrapolate ΔE^+_{DFT} to the standard hydrogen electrode $U_{SHE} = (\Phi - \Phi_{SHE})/e$, we use $\Phi_{SHE} =$ 4.44 eV that is measured experimentally[57]. Using the "corrected" activation energy, we define the DFT activation free energy ΔG^+_{DFT} as,

$$\Delta G^+_{DFT} = \Delta E^+_{DFT} + \Delta q\left[\frac{1}{2}\Delta\phi - (\phi_{SHE} - \phi_I)\right] + \Delta S^+. \tag{10}$$

Rossmeisl and collaborators posit that the main source of the activation entropy ΔS^{+} originates from the proton transfer across the Helmholtz layer plane, and not from any of the three HER elementary steps that take place at the electrode surface. Thus, ΔS^{+} is negligible in a low pH environment[58], as is the case in our study. Further, the pre-exponential factor for hydrogen recombination reaction $\frac{k_B T}{h}\exp(\frac{T\Delta S^{+}}{k_B T})$ is reported to be $\sim 10^{13}$ on several transition metal surfaces[59] suggesting also a nearly zero value for ΔS^{+}.

Data availability

The structures obtained from the simulations will be shared with community upon request.

Code availability

The VASP calculation inputs and outputs will be shared with community upon request.

Received: 20 July 2023; Accepted: 15 March 2024;
Published online: 08 May 2024

References

1. Adams, J. S., Kromer, M. L., Rodríguez-López, J. & flaherty, d. w. unifying concepts in electro- and thermocatalysis toward hydrogen peroxide production. *J. Am. Chem. Soc.* **143**, 7940–7957 (2021).
2. Wodrich, M. D., Fabrizio, A., Meyer, B. & Corminboeuf, C. Data-powered augmented volcano plots for homogeneous catalysis. *Chem. Sci.* **11**, 12070–12080 (2020).
3. Chen, Y., Chang, K.-H., Meng, F.-Y., Tseng, S.-M. & Chou, P.-T. Broadening the Horizon of the Bell–Evans–Polanyi Principle towards optically triggered structure planarization. *Angew. Chem. Int. Ed.* **60**, 7205–7212 (2021).
4. Ji, Q. et al. Revealing the Brønsted-Evans-Polanyi relation in halide-activated fast MoS2 growth toward millimeter-sized 2D crystals. *Sci. Adv.* **7**, eabj3274 (2021).
5. Göltl, F. & Mavrikakis, M. Generalized Brønsted-Evans-Polanyi relationships for reactions on metal surfaces from machine learning. *ChemCatChem.* **14**, e202201108 (2022).
6. Li, Y., Bahamon, D., Sinnokrot, M. & Vega, L. F. Computational screening of transition metal-doped CdS for photocatalytic hydrogen production. *npj Comput. Mater.* **8**, 229 (2022).
7. Zeng, Z. et al. Computational screening study of double transition metal carbonitrides M′2M″CNO2-MXene as catalysts for hydrogen evolution reaction. *npj Comput. Mater.* **7**, 80 (2021).
8. Mao, X. et al. Computational high-throughput screening of alloy nanoclusters for electrocatalytic hydrogen evolution. *npj Comput. Mater.* **7**, 46 (2021).
9. Evans, M. G. & Polanyi, M. Some applications of the transition state method to the calculation of reaction velocities, especially in solution. *Trans. Faraday Soc.* **31**, 875–894 (1935).
10. Evans, M. G. & Polanyi, M. Further considerations on the thermodynamics of chemical equilibria and reaction rates. *Trans. Faraday Soc.* **32**, 1333–1360 (1936).
11. Evans, M. G. & Polanyi, M. Inertia and driving force of chemical reactions. *Trans. Faraday Soc.* **34**, 11–24 (1938).
12. Bell, R. P. & Hinshelwood, C. N. The theory of reactions involving proton transfers. *Proc. R. Soc. Lond. Ser. A - Math. Phys. Sci.* **154**, 414–429 (1936).
13. Bronsted, J. N. Acid and basic catalysis. *Chem. Rev.* **5**, 231–338 (1928).
14. Brönsted, J. N. & Pedersen, K. Die katalytische Zersetzung des Nitramids und ihre physikalisch-chemische Bedeutung. *Z. f.ür. Physikalische Chem.* **108U**, 185–235 (1924).
15. Vojvodic, A., Hellman, A., Ruberto, C. & Lundqvist, B. I. From electronic structure to catalytic activity: a single descriptor for adsorption and reactivity on transition-metal carbides. *Phys. Rev. Lett.* **103**, 146103 (2009).
16. Zhdanov, V. P. Late stage of the formation of a protein corona around nanoparticles in biofluids. *Phys. Rev. E* **105**, 014402 (2022).
17. Santos, E., Lundin, A., Pötting, K., Quaino, P. & Schmickler, W. Model for the electrocatalysis of hydrogen evolution. *Phys. Rev. B* **79**, 235436 (2009).
18. Roy, S., Goedecker, S. & Hellmann, V. Bell-Evans-Polanyi principle for molecular dynamics trajectories and its implications for global optimization. *Phys. Rev. E* **77**, 056707 (2008).
19. Wang, S., Vorotnikov, V., Sutton, J. E. & Vlachos, D. G. Brønsted–Evans–Polanyi and transition state scaling relations of furan derivatives on Pd(111) and their relation to those of small molecules. *ACS Catal.* **4**, 604–612 (2014).
20. Sutton, J. E. & Vlachos, D. G. A theoretical and computational analysis of linear free energy relations for the estimation of activation energies. *ACS Catal.* **2**, 1624–1634 (2012).
21. Nørskov, J. K. et al. Universality in heterogeneous catalysis. *J. Catal.* **209**, 275–278 (2002).
22. Bligaard, T. et al. The Brønsted–Evans–Polanyi relation and the volcano curve in heterogeneous catalysis. *J. Catal.* **224**, 206–217 (2004).
23. Michaelides, A. et al. Identification of general linear relationships between activation energies and enthalpy changes for dissociation reactions at surfaces. *J. Am. Chem. Soc.* **125**, 3704–3705 (2003).
24. Wang, S. et al. Universal Brønsted-Evans-Polanyi relations for C–C, C–O, C–N, N–O, N–N, and O–O dissociation reactions. *Catal. Lett.* **141**, 370–373 (2011).
25. Liu, C., Liu, J. & Godin, R. ALD-Deposited NiO approaches the performance of platinum as a hydrogen evolution cocatalyst on carbon nitride. *ACS Catal.* **13**, 573–586 (2023).
26. Costabel, D. et al. Bridging platinum and palladium to bipyridine-annulated perylene for light-driven hydrogen evolution. *ACS Catal.* **13**, 7159–7169 (2023).
27. Nørskov, J. K. et al. Trends in the exchange current for hydrogen evolution. *J. Electrochem. Soc.* **152**, J23 (2005).
28. Cheng, Y.-L. et al. Examination of the Brønsted–Evans–Polanyi relationship for the hydrogen evolution reaction on transition metals based on constant electrode potential density functional theory. *Phys. Chem. Chem. Phys.* **24**, 2476–2481 (2022).
29. Tang, M. T., Liu, X., Ji, Y., Norskov, J. K. & Chan, K. Modeling hydrogen evolution reaction kinetics through explicit water–metal interfaces. *J. Phys. Chem. C.* **124**, 28083–28092 (2020).
30. Zheng, J., Sheng, W., Zhuang, Z., Xu, B. & Yan, Y. Universal dependence of hydrogen oxidation and evolution reaction activity of platinum-group metals on pH and hydrogen binding energy. *Sci. Adv.* **2**, e1501602 (2016).
31. Zeradjanin, A. R., Narangoda, P., Masa, J. & Schlögl, R. What controls activity trends of electrocatalytic hydrogen evolution reaction?—Activation Energy Versus Frequency Factor. *ACS Catal.* **12**, 11597–11605 (2022).
32. Safizadeh, F., Ghali, E. & Houlachi, G. Electrocatalysis developments for hydrogen evolution reaction in alkaline solutions – A Review. *Int. J. Hydrog. Energy* **40**, 256–274 (2015).
33. Bard, A. J. & Faulkner, L. R. *Electrochemical Methods - Fundamentals and Applications.* (John Wiley & Sons, Inc., 2001).
34. Eyring, H. The Activated Complex in Chemical Reactions. *J. Chem. Phys.* **3**, 107–115 (1935).
35. Eyring, H. Viscosity, plasticity, and diffusion as examples of absolute reaction rates. *J. Chem. Phys.* **4**, 283–291 (1936).
36. Zhu, H. et al. Atomic-scale core/shell structure engineering induces precise tensile strain to boost hydrogen evolution catalysis. *Adv. Mater.* **30**, 1707301 (2018).
37. Yang, T. T. & Saidi, W. A. Reconciling the volcano trend with the butler–volmer model for the hydrogen evolution reaction. *J. Phys. Chem. Lett.* **13**, 5310–5315 (2022).

38. Skúlason, E. et al. Density functional theory calculations for the hydrogen evolution reaction in an electrochemical double layer on the Pt(111) electrode. *Phys. Chem. Chem. Phys.* **9**, 3241–3250 (2007).
39. Yang, T. T., Patil, R. B., McKone, J. R. & Saidi, W. A. Revisiting trends in the exchange current for hydrogen evolution. *Catal. Sci. Technol.* **11**, 6832–6838 (2021).
40. Yang, T. T. & Saidi, W. A. Simple approach for reconciling cyclic voltammetry with hydrogen adsorption energy for hydrogen evolution exchange current. *J. Phys. Chem. Lett.* **14**, 4164–4171 (2023).
41. Rossmeisl, J., Skúlason, E., Björketun, M. E., Tripkovic, V. & Nørskov, J. K. Modeling the electrified solid–liquid interface. *Chem. Phys. Lett.* **466**, 68–71 (2008).
42. Wen, Y. & Zhang, J. J. S. S. C. Surface energy calculation of the fcc metals by using the MAEAM. *Solid State Commun.* **144**, 163–167 (2007).
43. Zhang, J.-M., Wang, D.-D. & Xu, K.-W. Calculation of the surface energy of hcp metals by using the modified embedded atom method. *Appl. Surf. Sci.* **253**, 2018–2024 (2006).
44. Hofmann, P. The surfaces of bismuth: Structural and electronic properties. *Prog. Surf. Sci.* **81**, 191–245 (2006).
45. Eigen, M. Proton transfer, acid-base aatalysis, and enzymatic hydrolysis. *Angew. Chem. Int Ed. Engl.* **3**, 72 (1964).
46. Ogasawara, H. et al. Structure and bonding of water on Pt(111). *Phys. Rev. Lett.* **89**, 276102 (2002).
47. Van den Bossche, M., Skúlason, E., Rose-Petruck, C. & Jónsson, H. Assessment of constant-potential implicit solvation calculations of electrochemical energy barriers for H2 evolution on Pt. *J. Phys. Chem. C.* **123**, 4116–4124 (2019).
48. Chan, K. & Nørskov, J. K. Potential dependence of electrochemical barriers from ab initio calculations. *J. Phys. Chem. Lett.* **7**, 1686–1690 (2016).
49. Tymoczko, J., Calle-Vallejo, F., Schuhmann, W. & Bandarenka, A. S. Making the hydrogen evolution reaction in polymer electrolyte membrane electrolysers even faster. *Nat. Commun.* **7**, 10990 (2016).
50. Yang, T. T. et al. Computationally guided design to accelerate discovery of doped β-Mo2C catalysts toward hydrogen evolution reaction. *ACS Catal.* **12**, 11791–11800 (2022).
51. Jaramillo, T. F. et al. Identification of Active Edge Sites for Electrochemical H2 Evolution from MoS2 Nanocatalysts. *Science* **317**, 100–102 (2007).
52. Zheng, Y. et al. Hydrogen evolution by a metal-free electrocatalyst. *Nat. Commun.* **5**, 3783 (2014).
53. Yang, T. T. & Saidi, W. A. Tuning the hydrogen evolution activity of β-Mo2C nanoparticles via control of their growth conditions. *Nanoscale* **9**, 3252–3260 (2017).
54. Chase, M. W. et al. JANAF Thermochemical Tables, 1982 Supplement. *J. Phys. Chem. Ref. Data* **11**, 695 (1982).
55. Henkelman, G., Uberuaga, B. P. & Jo´nsson, H. A climbing image nudged elastic band method for finding saddle points and minimum energy paths. *J. Chem. Phys.* **113**, 9901 (2000).
56. Skúlason, E. et al. Modeling the electrochemical hydrogen oxidation and evolution reactions on the basis of density functional theory calculations. *J. Phys. Chem. C.* **114**, 18182–18197 (2010).
57. Trasatti, S. The Absolute electrode potential: ab explanatory note. *Pure AppL. Chem.* **58**, 955–966 (1986).
58. Rossmeisl, J., Chan, K., Skúlason, E., Björketun, M. E. & Tripkovic, V. On the pH dependence of electrochemical proton transfer barriers. *Catal. Today* **262**, 36–40 (2016).
59. Masel, R. I. Principles of adsorption and reaction on solid surfaces. *Wiley-Interscience 1st edition* (1996). ISBN-13: 978-0471303923.

Acknowledgements

We acknowledge partial financial support from the National Science Foundation (Award No. CBET-2130804). Computational support was provided in part by the University of Pittsburgh Center for Research Computing through the resources provided on the H2P cluster, which is supported by NSF (Award No. OAC-2117681).

Author contributions

T.Y. and W.A.S. conceived the project. T.Y carried out the DFT calculations and analyzed the results. T.Y. wrote the manuscript under the direction of W.A.S.

Competing interests

The authors declare no competing interests.

Additional information

Supplementary information The online version contains supplementary material available at https://doi.org/10.1038/s41524-024-01244-3.

Correspondence and requests for materials should be addressed to Wissam A. Saidi.